Kinetics and Mechanisms of Heterogeneous Reaction of Gaseous Hydrogen Peroxide on Mineral Oxide Particles

ARTICLE *in* ENVIRONMENTAL SCIENCE & TECHNOLOGY · APRIL 2011

Impact Factor: 5.33 · DOI: 10.1021/es104107c · Source: PubMed

4 AUTHORS, INCLUDING:

Yan Zhao
Université de Versailles Saint-Quentin
753 PUBLICATIONS **5,390** CITATIONS
SEE PROFILE

Xiaoli Shen
Karlsruhe Institute of Technology
3 PUBLICATIONS **57** CITATIONS
SEE PROFILE

Xuan Zhang
Aerodyne Research Inc.
19 PUBLICATIONS **205** CITATIONS
SEE PROFILE

Environmental Science & Technology

ARTICLE

pubs.acs.org/est

Kinetics and Mechanisms of Heterogeneous Reaction of Gaseous Hydrogen Peroxide on Mineral Oxide Particles

Yue Zhao, Zhongming Chen,* Xiaoli Shen, and Xuan Zhang

State Key Laboratory of Environmental Simulation and Pollution Control, College of Environmental Sciences and Engineering, Peking University, Beijing 100871, China

Supporting Information

ABSTRACT: Recent studies have shown that heterogeneous reactions of hydrogen peroxide (H_2O_2) on aerosol surfaces may play an important role in tropospheric chemistry. The data concerning the kinetics and mechanisms of these reactions, however, are quite scarce so far. Here, we investigated, for the first time, the heterogeneous reactions of gaseous H_2O_2 on SiO_2 and α-Al_2O_3 particles, two major components of mineral dust aerosol, using transmission-Fourier Transform Infrared (T-FTIR) spectroscopy, and high-performance liquid chromatography (HPLC). It is found that H_2O_2 molecularly adsorbs on SiO_2, and a small amount of molecularly adsorbed H_2O_2 decomposes due to its thermal instability. For α-Al_2O_3, catalytic decomposition of H_2O_2 evidently occurs, but there is also a small amount of H_2O_2 molecularly adsorbed on the particle surface. The BET uptake coefficients of H_2O_2 on both particles appear to be independent of gaseous H_2O_2 concentration (1.27−13.8 ppmv) and particle sample mass (2.8−6.5 mg for SiO_2 and 8.6−18.9 mg for α-Al_2O_3), but are strongly dependent on relative humidity with the values ranging from $(1.55 \pm 0.14) \times 10^{-8}$ and $(1.21 \pm 0.04) \times 10^{-7}$ at 2% RH to $(0.61 \pm 0.06) \times 10^{-8}$ and $(0.76 \pm 0.09) \times 10^{-7}$ at 76% RH for SiO_2 and α-Al_2O_3, respectively. On the basis of the experimental results and literature data, the potential mechanisms for heterogeneous decomposition of H_2O_2 were proposed, and the atmospheric implications of these reactions were discussed. It is found that heterogeneous reaction of H_2O_2 on both mineral oxides plays a significant role in processing mineral aerosols, although its role as a sink for ambient H_2O_2 is probably limited.

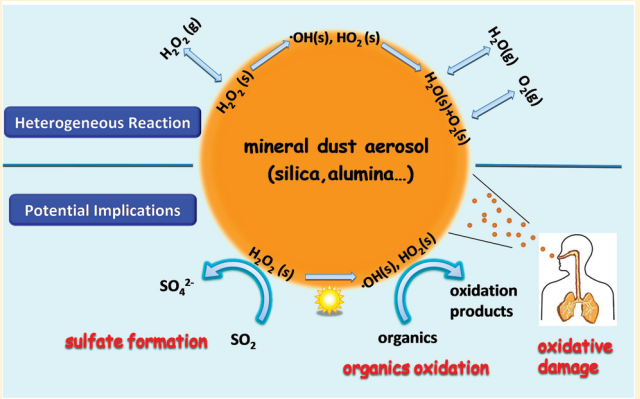

INTRODUCTION

Atmospheric hydrogen peroxide (H_2O_2) is a key product of photochemistry in the atmosphere, primarily arising from the bimolecular recombination of hydroperoxy (HO_2) radicals.[1−3] As a reservoir of odd-hydrogen radicals (OH and HO_2), the formation and destruction of H_2O_2 are intimately linked to the HO_x radicals cycling and O_3 production.[1−3] Additionally, due to high water solubility, H_2O_2 can act as an important oxidant in atmospheric aqueous systems such as cloud, fog, and rainwater, where it substantially contributes to the formation of secondary sulfate and may play a potentially important role in the formation of secondary organic aerosol.[4,5]

Recent field and model combined studies demonstrated that gaseous H_2O_2 concentrations in a Saharan dust plume [6] and in the Arctic spring troposphere [7] were largely overpredicted by a standard gas-phase chemical mechanism, whereas after incorporating the heterogeneous uptake of H_2O_2 and/or HO_2 on aerosol surfaces into the model, the observed and modeled values were in good agreement. Our recent field study of atmospheric peroxides in Beijing has also provided the evidence showing that the heterogeneous removal of H_2O_2 on aerosol surfaces is important.[8]

Mineral dust aerosol comprises a significant fraction of atmospheric particulate matter, with a global emission flux of 1000−3000 Tg/yr.[9] Both field and model studies suggested that there existed strong interactions between atmospheric trace gases with the long-range transported mineral dust aerosols.[6,9,10] Over the past two decades, special emphasis of laboratory studies has been given to the heterogeneous uptake kinetics and reaction mechanisms of reactive gaseous species such as nitrogen oxides, nitric acid, sulfur oxides, ozone, and organics on various mineral aerosols (see the reviews in refs 11 and 12). However, laboratory studies addressing the heterogeneous reaction of gaseous H_2O_2 with mineral dust have received less attention so far.

Quite recently, Pradhan et al. [13,14] have studied the uptake of gaseous H_2O_2 by TiO_2 and authentic dust aerosols using an aerosol flow tube (AFT) coupled with a chemical ionization mass spectrometry (CIMS), and reported a series of uptake coefficients over a wide range of relative humidity (RH). Nonetheless,

Received: December 8, 2010
Accepted: March 15, 2011
Revised: March 9, 2011
Published: March 23, 2011

information on the kinetics of heterogeneous reactions of H_2O_2 with mineral dust aerosols is still limited, and more kinetic data involving other mineral aerosols of interest will enable us to better evaluate the potential impacts of heterogeneous reactions of H_2O_2 on tropospheric chemistry. In addition, the reaction mechanism of H_2O_2 with mineral dust aerosol remains uncertain and thereby requires further study.

SiO_2 and α-Al_2O_3 are two typical components of mineral dust and are widely used as model particles for studying heterogeneous reactions with atmospheric trace gases. In the present study, heterogeneous reactions of gaseous H_2O_2 on SiO_2 and α-Al_2O_3 were investigated using transmission-Fourier Transform Infrared (T-FTIR) spectroscopy and high-performance liquid chromatography (HPLC). The spectroscopic and chromatographic data were analyzed and interpreted to derive the uptake kinetics of H_2O_2 on both oxides, and to provide some insight into the reaction mechanisms. The effect of water on heterogeneous reactions was explored under a full range of RH conditions. Potential atmospheric implications of these reactions were discussed.

EXPERIMENTAL SECTION

Materials. The SiO_2 powder (Alfa Aesar, 99.9%), ∼5.5 mg, with particle size around 80 nm, and the α-Al_2O_3 powder (Alfa Aesar, 99.9%), ∼15.5 mg, with particle size around 35 nm were used in this study. The Brunauer−Emmett−Teller (BET) surface area of SiO_2 and α-Al_2O_3 samples was measured to be 440(±12) $m^2\ g^{-1}$ and 32.8(±1.6) $m^2\ g^{-1}$, respectively, using a Micromeritics ASAP 2010 BET apparatus. Aqueous solution of H_2O_2 (Sigma-Aldrich, 50 wt %) and H_3PO_4 (Sigma-Aldrich, 85% for HPLC), N_2 (≥99.999%, Beijing Pryx Applied Gas Company Limited), and O_2 (≥99.999%, Beijing Analytical Instrument Factory) were also used in this work.

T-FTIR Experiments. The heterogeneous reactions were performed in a flow reactor, which has been described previously.[15] Briefly, the flow reactor (length 15 cm, i.d. 3.3 cm) is a quartz cylinder. The particle samples were directly placed on a 250-mesh stainless steel circular grid and compressed to form a solid coating, which was then mounted in the center of the reactor. Under typical experimental conditions, the flow reactor was maintained at room temperature and ambient pressure. The H_2O_2-containing simulated air was introduced into the reactor at a constant flow rate of 400 sccm, which leads to laminar flow conditions in the flow reactor (Reynolds number = 17). A FTIR spectrometer (Nicolet 6700, Thermo Scientific) equipped with a mercury−cadmium−telluride (MCT) detector was employed to record the infrared spectra in the frequency range of 4000 to 400 cm^{-1}. All spectra were collected at a resolution of 4 cm^{-1}, and 32 scans were averaged for each spectrum corresponding to a time resolution of 19 s.

Prior to each heterogeneous reaction, the particle sample was evacuated at 298 ± 1 K for 30 min to remove the physisorbed water and other impurities as much as possible. The particle sample was then exposed to the simulated air at different RH for 30 min. The RH was measured by a hygrometer (Vaisala HMT100) with the uncertainty of ±1.7%. Subsequently, the H_2O_2-containing simulated air (20% O_2 and 80% N_2) was introduced into the reactor at a flow rate of 400 sccm and the T-FTIR spectra were recorded. Each spectrum was referenced to the spectrum of particles in equilibrium with water vapor. At the exit of the flow reactor, the 400 sccm air stream was drawn into a thermostatically controlled scrubbing coil collector maintained at 277 K, and the 1 mM H_3PO_4 solution, used as the stripping solution, was delivered into the collector by an HPLC pump at a flow rate of 0.2 mL min^{-1} to collect the gas-phase H_2O_2. The resulting solution was then immediately analyzed with a HPLC instrument described below. The collection efficiency of the coil for H_2O_2 was determined to be ≥98%,[5] and details about this collection system can be found in our previous work.[5] After the reaction, adsorbed H_2O_2 on the particle samples was immediately extracted in 1 mM H_3PO_4 solution maintained at 277 K. The resulting solution was filtered and then analyzed with HPLC.

Generation of Gaseous H_2O_2. The 50 wt % H_2O_2 solution was processed to generate gaseous H_2O_2. Details are described in the Supporting Information.

H_2O_2 Detection. H_2O_2 was determined using a HPLC instrument (Agilent 1200, USA) equipped with a fluorescent detector, with postcolumn derivation involving the hemin-catalyzed oxidation of H_2O_2 to a fluorescent derivative by hydroxyphenylacetic acid. The details about the analysis method can be seen in our previous study.[5] The detection limit for H_2O_2 in 1 mM H_3PO_4 solution is 0.04 μM, which corresponds to 0.45 ppbv in the 400 sccm simulated air.

RESULTS AND DISCUSSION

T-FTIR Measurements of H_2O_2 Uptake on SiO_2 and α-Al_2O_3. It should be noted that the gaseous H_2O_2-containing flow generated here also contains a relatively high partial pressure of water vapor, which accounts for approximately 2% RH in the 400 sccm simulated air. As shown in Figure S1 of the Supporting Information, the strong absorption bands assigned to adsorbed water were observed in the T-FTIR spectra of SiO_2 and α-Al_2O_3 exposed to gaseous H_2O_2. Because water adsorption on both particles almost reaches the equilibrium, whereas the amount of molecularly adsorbed H_2O_2 is negligible at 20 s, the spectrum collected at 20 s has been subtracted from the spectra shown in Figure S1 of the Supporting Information, to avoid the disturbance from the absorption bands of adsorbed water on those of adsorbed H_2O_2.

Figure 1 shows the subtracted T-FTIR spectra of H_2O_2 adsorption on SiO_2 and α-Al_2O_3 at 6% RH as a function of time. Upon H_2O_2 uptake on particle surfaces, several absorption bands appear and grow in intensity with increasing time. The assignments of these bands based on literature data are presented in Table 1. It is evident that there is a considerable amount of H_2O_2 molecularly adsorbed on SiO_2 and α-Al_2O_3. This observation is well supported by the appreciable quantity of H_2O_2 molecules on particle surfaces determined with HPLC. The negative bands at 3661 cm^{-1} and 3696 cm^{-1}, assigned to isolated OH groups on SiO_2 and α-Al_2O_3 respectively decrease in intensity with exposure time, implying that surface isolated OH groups are the reactive sites for molecular adsorption of H_2O_2 on both particles. It can be also observed that there is another negative feature at 1630 cm^{-1} for SiO_2 and 1652 cm^{-1} for α-Al_2O_3. This feature is associated with the bending vibration of surface adsorbed water and the decrease in peak intensity is possibly due to an interaction with molecularly adsorbed H_2O_2.

It is worthy noting that there are two bending vibrations observed for the O−O−H group of H_2O_2 adsorbed on α-Al_2O_3, whereas only one of that for H_2O_2 on SiO_2. This may be ascribed to different types of H-bond between adsorbed H_2O_2 and the particle surface. As suggested by Żegliński et al.,[17] the bending vibrations around 1332 cm^{-1} are probably associated with the O−O−H group, where only the oxygen participates the formation of H-bond with surface isolated OH groups, whereas the bending

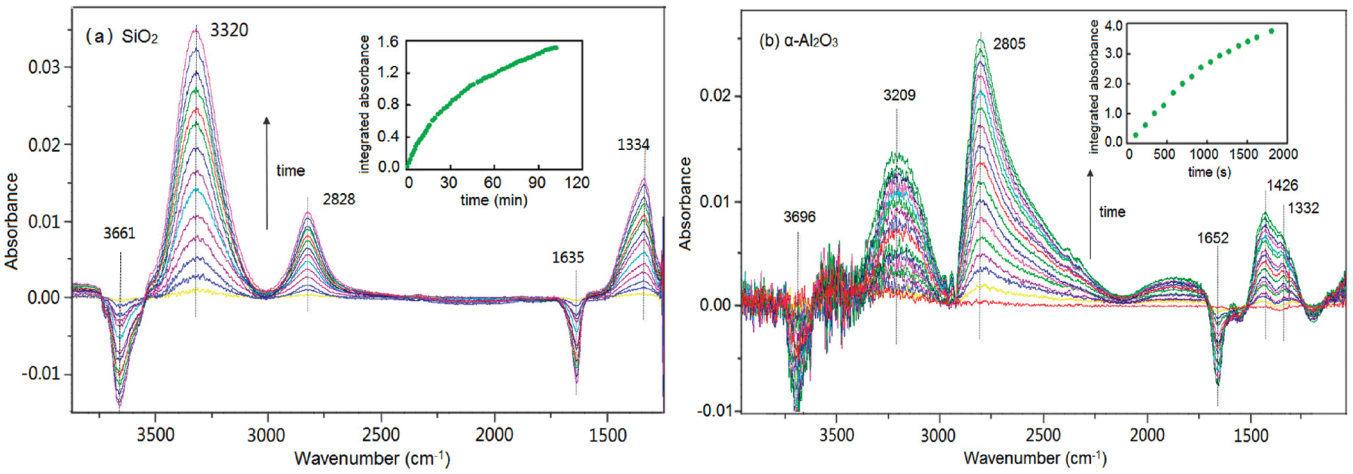

Figure 1. T-FTIR spectra of the heterogeneous uptake of H_2O_2 on (a) SiO_2 and (b) α-Al_2O_3 at 6%RH and $[H_2O_2] = 2.41 \times 10^{14}$ molecules cm^{-3}. The inset shows the temporal evolution of the integrated absorbance around 2828 cm^{-1} and 2805 cm^{-1} for molecularly adsorbed H_2O_2 on SiO_2 and α-Al_2O_3, respectively.

Table 1. Assignment of the Absorption Bands in the Spectra Shown in Figure *1*

particle	peak position	assignment	ref
SiO_2	3661	stretching of surface isolated OH group	16
	3320	stretching of OH in H_2O_2 (ν_1)	17
	2828	bending overtone of H_2O_2 ($2\nu_6$)	17−19
	1635	bending of H_2O	
	1334	bending of OOH in H_2O_2 (ν_6)	17
α-Al_2O_3	3696	stretching of surface isolated OH group	16
	3209	stretching of OH in H_2O_2 (ν_1)	18,19
	2805	combination of bending overtones of H_2O_2 ($2\nu_2$, $2\nu_6$, $\nu_2+\nu_6$)	18,19
	1652	bending of H_2O	
	1426	bending of OOH in H_2O_2 (ν_2)	17−19
	1332	bending of OOH in H_2O_2 (ν_6)	17−19

vibration at 1425 cm^{-1} is likely linked to the O−O−H group where the hydrogen is also involved in H-bond, probably interacting with the oxygen of the surface OH or Al−O group. This discrepancy in H-bond may indicate the different surface reactivity of SiO_2 and α-Al_2O_3 toward H_2O_2.

In addition, T-FTIR experiments upon varying RH were also performed to investigate the effect of water vapor on H_2O_2 uptake on SiO_2 and α-Al_2O_3. As shown in Figure S2 of the Supporting Information, there is little change in the spectrum collected when the amount of molecularly adsorbed H_2O_2 reached the maximum at different RH, except for the decrease of the absorbance with increasing RH. This indicates that H_2O_2 adsorption can be greatly suppressed by surface adsorbed water.

Uptake Kinetics of H_2O_2 on SiO_2 and α-Al_2O_3. It should be mentioned that T-FTIR experiments appear to provide information on only the molecularly adsorbed H_2O_2 on SiO_2 and α-Al_2O_3. However, the α-Al_2O_3 surface is highly reactive toward various trace gases,[11,12,20] and even the relatively inactive SiO_2 surface was found to enable the thermal decomposition of H_2O_2 in aqueous system.[21] The decomposition of H_2O_2, therefore, is expected to occur on SiO_2 and α-Al_2O_3.

To figure out whether the decomposition of H_2O_2 occurs on oxide surfaces, the total uptake of H_2O_2 (namely the H_2O_2 loss from the gas phase) was determined by monitoring the gas-phase H_2O_2 concentration at the exit of the flow reactor using HPLC coupled with an online H_2O_2 collector, which was described in detail in our previous work.[5] Figure 2 illustrates the typical kinetic curves of the total uptake of H_2O_2 on SiO_2 and α-Al_2O_3 as a function of exposure time at 6% RH and 2.41×10^{14} molecules cm^{-3} of H_2O_2, and the molecularly adsorbed H_2O_2, determined using the integrated absorbance around 2828 cm^{-1} and 2805 cm^{-1} for H_2O_2 on both particles respectively for the same kinetic run was also displayed here for comparison. The calibration of integrated absorbance can be found in the Supporting Information. It is notable that the amount of molecularly adsorbed H_2O_2 only accounts for approximately 53% and 29% of the H_2O_2 loss from the gas phase due to the uptake by SiO_2 and α-Al_2O_3 respectively implying that a considerable amount of H_2O_2 does decompose on both particles. However, owing to the larger intrinsic reactivity of the α-Al_2O_3 surface, the decomposition of H_2O_2 on α-Al_2O_3 occurs to a much severer extent than that on SiO_2.

The reactivity of α-Al_2O_3 toward H_2O_2 can also be characterized in terms of a turnover number,[22] T_N:

$$T_N = \frac{\text{the number of } H_2O_2 \text{ molecules lost from the gas phase}}{\text{the number of available surface sites}} \quad (1)$$

The total number of available surface sites for α-Al_2O_3 is estimated from the sample mass and the BET surface area, with a surface site density of 4×10^{14} sites cm^{-2}.[23] A turnover number greater than one indicates that the surface is not saturated and that the reaction process is catalytic, involving the regeneration of surface active sites.[22] At RH of 6% and gaseous H_2O_2 concentration of 3.39×10^{14} molecules cm^{-3}, the total uptake of H_2O_2 by alumina particles was determined to be 4.1×10^{18} molecules m^{-2} at 20 min of exposure, leading to a turnover number of 1.03. On a longer time scale, the turnover number is expected to be much larger (Figure S3 of the Supporting Information). This result demonstrates that the heterogeneous decomposition of H_2O_2 on α-Al_2O_3 appears to be catalytic.

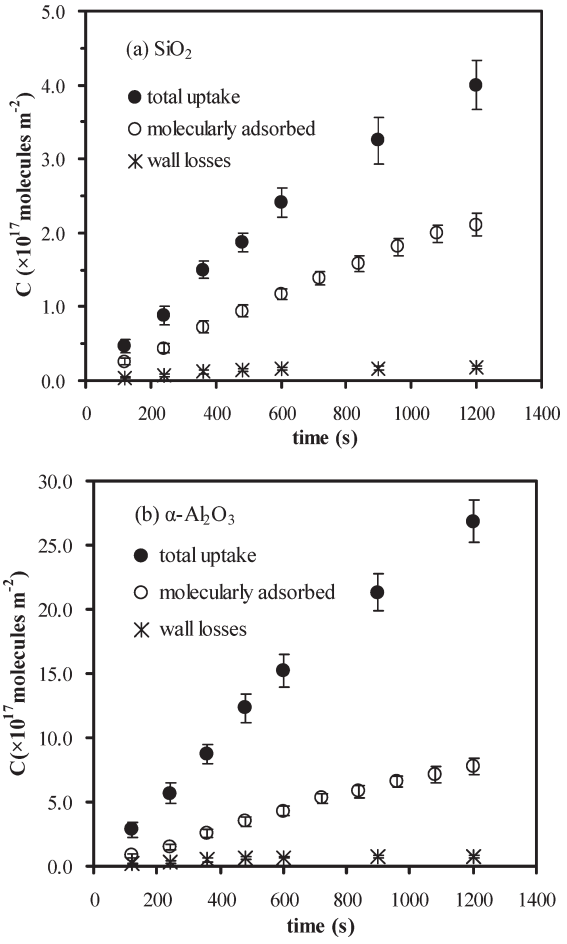

Figure 2. Typical kinetic curves of H_2O_2 uptake on the surface of (a) SiO_2 and (b) α-Al_2O_3 at 6% RH and $[H_2O_2] = 2.41 \times 10^{14}$ molecules cm^{-3}. The total uptake of H_2O_2 by SiO_2 and α-Al_2O_3 was obtained by subtracting the H_2O_2 wall losses, which was measured in the absence of particle samples, from the H_2O_2 losses in the presence of particles. The uptake data were normalized by the BET surface area of the particle samples.

To further examine the uptake capability of H_2O_2 on SiO_2 and α-Al_2O_3, the uptake coefficient (γ) of H_2O_2 was calculated by eqs 2 and 3:[15,20]

$$\gamma = \frac{d\{C\}/dt}{Z} \quad (2)$$

$$Z = \frac{1}{4}A_s[C]\sqrt{\frac{8RT}{\pi M_c}} \quad (3)$$

where $\{C\}$ is the total uptake of H_2O_2 by particle surfaces, $[C]$ is the gaseous H_2O_2 concentration, Z is collision frequency, M_c is the molecular weight of H_2O_2, and A_s is the effective surface area of the particles. Here, the uptake rates ($d\{C\}/dt$) of H_2O_2 on both particles were determined from the gradients of linear least-squares fits to the data points within 10 min of exposure (Figure 2). Considering that on the time scales that kinetic parameters are evaluated H_2O_2 may be accessible to the entire sample, the BET surface area of the sample is used to calculate the γ. Under typical experimental conditions of 6%RH and $[H_2O_2] = 2.41 \times 10^{14}$ molecules cm^{-3}, the γ of H_2O_2 on SiO_2 and α-Al_2O_3 was calculated to be $(1.46 \pm 0.13) \times 10^{-8}$ and $(1.05 \pm 0.06) \times 10^{-7}$, respectively.

To further confirm the true surface area for H_2O_2 uptake, the uptake coefficients of H_2O_2 on both particles were measured as a function of sample mass. The BET uptake coefficients of H_2O_2 on both particles appear to be independent of the sample mass (Figure S4 of the Supporting Information), implying that the BET surface area seems to more appropriately represent the effective surface area of the particle samples. It should be noted that the uptake experiments were performed at relative high H_2O_2 pressures, and on a few minutes time scale the initial uptake processes are already achieved. Therefore, the observed uptake coefficients represent the steady state rather than the initial state.

Furthermore, the heterogeneous rate laws were also investigated by performing measurements over the H_2O_2 concentration range of $(0.31-3.39) \times 10^{14}$ molecules cm^{-3} (1.27−13.8 ppmv) at 6% RH. Part a of Figure S5 of the Supporting Information shows the uptake rates of H_2O_2 on SiO_2 and α-Al_2O_3 versus the corresponding H_2O_2 concentrations on a double-logarithmic scale. The linear relationships between the uptake rates and H_2O_2 concentrations with the gradients of 0.965 ± 0.091 and 0.973 ± 0.082 were observed on SiO_2 and α-Al_2O_3 respectively suggesting the first-order rate laws for H_2O_2 uptake on both particles within the concentration range given. The BET uptake coefficients of H_2O_2 on both particles appear to be independent of H_2O_2 concentration, with the average values of $(1.47 \pm 0.12) \times 10^{-8}$ for SiO_2 and $(0.99 \pm 0.08) \times 10^{-7}$ for α-Al_2O_3 (part b of Figure S5 of the Supporting Information).

Recently, Pradhan et al. [13,14] reported a series of uptake coefficients of gaseous H_2O_2 on TiO_2 and authentic dust aerosols. The values of γ there were over 3 orders of magnitude higher than our results. Generally, the TiO_2 surface has higher intrinsic reactivity than the α-Al_2O_3 surface, as suggested by the higher uptake coefficients of various gaseous species on TiO_2 compared to those on α-Al_2O_3.[11] In addition to silica and alumina, Saharan dust and Gobi sand also contain a considerable amount of Fe_2O_3 and MgO, and a small amount of CaO and/or TiO_2. These oxides generally display higher reactivity toward various reactive species than silica and alumina.[11,24,25] Particularly, iron oxide is recognized to be highly effective for the catalytic decomposition of H_2O_2.[26] Overall, the authentic dust aerosols are expected to be more reactive toward H_2O_2.

On the other hand, the heterogeneous uptake of H_2O_2 on TiO_2 and authentic dust aerosols were explored using AFT-CIMS at relative lower H_2O_2 pressures, and the time scale for kinetic parameter evaluation is a few seconds, which is short enough to observe the initial uptake process. Therefore, the γ reported by Pradhan et al. should represent the initial state. However, as discussed above, the γ measured in our study seems to be the steady state. Generally, the initial γ values are expected to be much larger than the steady state values. For example, in a Knudsen-MS study by Michel et al.,[24] the initial γ of O_3 on Saharan dust and α-Fe_2O_3 were determined to be an order of magnitude larger than the steady state values.

Effect of Water on H_2O_2 Uptake on SiO_2 and α-Al_2O_3. The effect of water on H_2O_2 uptake was investigated between 2% and 76% RH at $[H_2O_2] = 2.41 \times 10^{14}$ molecules cm^{-3}. H_2O_2 wall losses in the reactor and air sampling line under different humidities were also measured in the absence of particles (Figure S6 of the Supporting Information). By subtracting these background values from H_2O_2 losses from the gas phase in the presence of particles, the total uptake of H_2O_2 by SiO_2 and

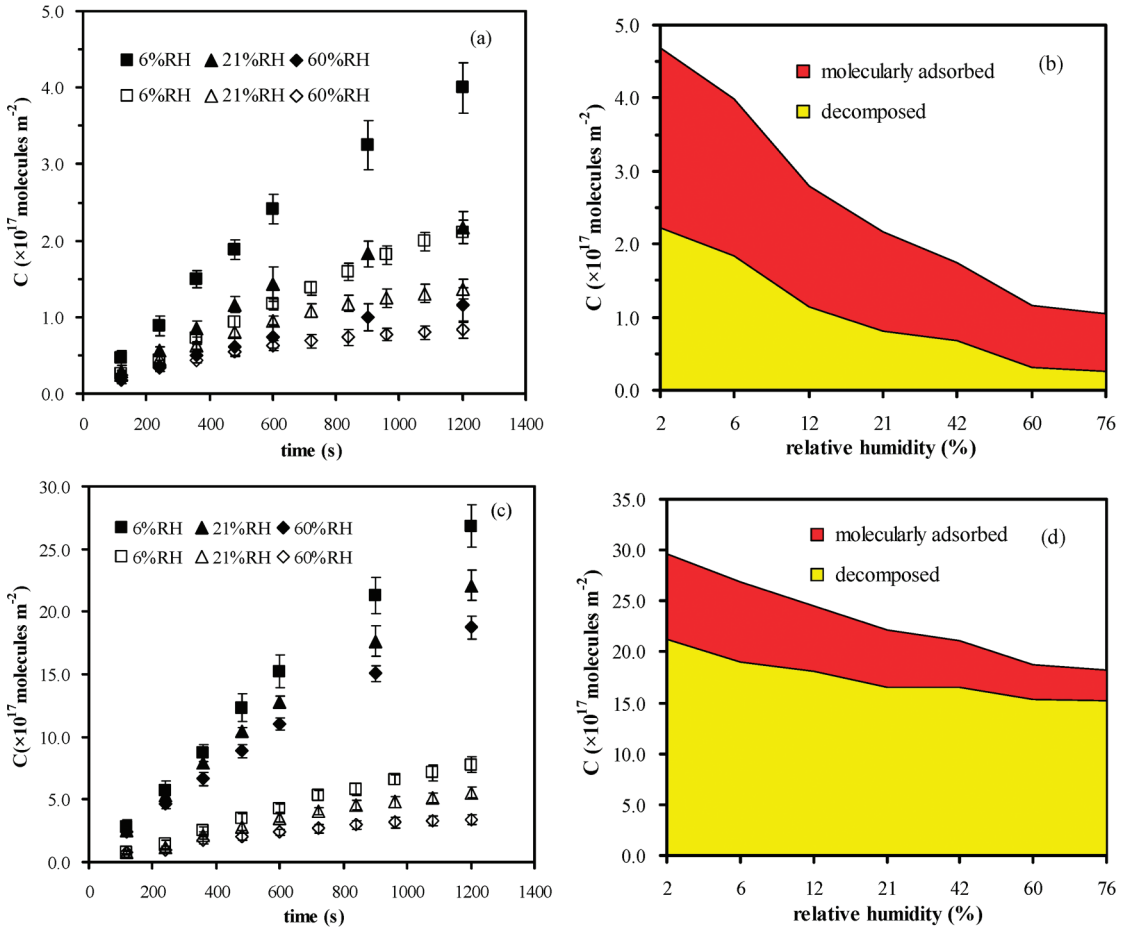

Figure 3. Relative humidity dependence of total H_2O_2 uptake (including molecularly adsorbed and decomposed H_2O_2) on the surface of (a, b) SiO_2 and (c, d) α-Al_2O_3 at $[H_2O_2] = 2.41 \times 10^{14}$ molecules cm^{-3}. a and c, the temporal evolution of H_2O_2 uptake by the particles at different RH, the filled and open markers refer to the total uptake, and molecularly adsorbed H_2O_2, respectively; b and d, the total amount of molecularly adsorbed and decomposed H_2O_2 at 20 min of exposure as a function of RH. The uptake data were normalized by the BET surface area of the particle samples.

α-Al_2O_3 were then obtained. As demonstrated in Figure 3, the total uptake of H_2O_2 on both particles decreased markedly with increasing RH. On SiO_2, the thermal decomposition of molecularly adsorbed H_2O_2 becomes less efficient at higher RH, with the proportion to the total uptake decreasing from 41% at 12% RH to 20% at 76% RH. This implies water may play a role in stabilizing the molecularly adsorbed H_2O_2 on SiO_2.[17] As for α-Al_2O_3, the catalytic decomposition still dominates H_2O_2 uptake even at high RH probably due to its high surface reactivity.

In addition, humidity dependence of the γ for H_2O_2 on both particles was also investigated. As shown in Figure 4, the γ of H_2O_2 on SiO_2 decreases from $(1.55 \pm 0.14) \times 10^{-8}$ to $(0.81 \pm 0.11) \times 10^{-8}$ with increasing RH in the range of 2−21%, whereas it appears to remain at a constant value at RH > 21%. A similar trend was observed for H_2O_2 uptake on α-Al_2O_3 with the γ value ranging from $(1.21 \pm 0.04) \times 10^{-7}$ for 2% RH to $(0.84 \pm 0.07) \times 10^{-7}$ for 21% RH and then approaching a low limiting value of $(0.72 \pm 0.04) \times 10^{-7}$ for RH ≥ 42%.

It is evident from Figures 3 and 4 that adsorbed water significantly suppresses H_2O_2 uptake on SiO_2 and α-Al_2O_3, suggesting that water can compete for the same surface sites for the adsorption and decomposition of H_2O_2. As discussed above, surface OH groups are the surface sites for the molecular adsorption of H_2O_2 on SiO_2 and α-Al_2O_3, thus the formation of surface OH groups should facilitate the H_2O_2 adsorption, whereas the depletion of surface OH groups should inhibit this process. Both SiO_2 and α-Al_2O_3 surfaces are quickly hydroxylated after contact with water vapor, resulting in an OH-terminated surface, on top of which additional water can then molecularly adsorb.[27,28] It should be mentioned that the SiO_2 and α-Al_2O_3 samples used in our measurements may have already been hydroxylated, and the evacuation pretreatment at room temperature can not remove the hydroxylation layer. Therefore, under humid conditions (2% to 76% RH), water molecularly adsorbs on the hydroxylated oxide surfaces to consume the surface OH groups and thus suppresses the molecular adsorption of H_2O_2. At the same time, the thermal decomposition of molecularly adsorbed H_2O_2 on SiO_2 also decreases markedly with increasing RH (Figure 3), probably due to the stabilization effect of water. Furthermore, because of depletion of other reactive sites on α-Al_2O_3 surfaces, such as acidic Al and basic O sites, the catalytic decomposition of H_2O_2 is also greatly suppressed by adsorbed water. Overall, the competitive consumption of the surface sites on SiO_2 and α-Al_2O_3 surfaces by adsorbed water results in the γ decreasing with increasing RH.

It is reported that approximately one monolayer of water molecules adsorbs on SiO_2 and α-Al_2O_3 at RH around 20%, and multilayers adsorption of water occurs at higher RH.[25,27,28] At RH < 20%, the increasing submonolayer coverage of water

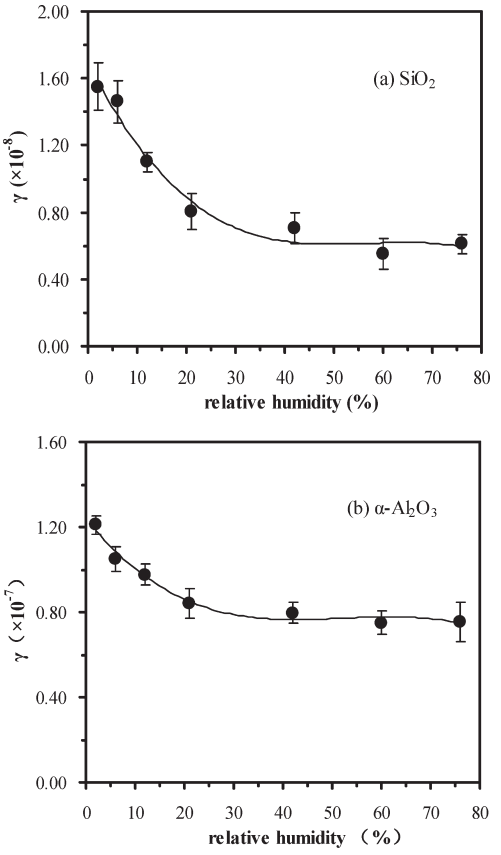

Figure 4. BET uptake coefficients of H_2O_2 on (a) SiO_2 and (b) α-Al_2O_3 as a function of RH at $[H_2O_2] = 2.41 \times 10^{14}$ molecules cm^{-3}.

significantly competes for the surface sites, whereas at higher RH the consumption of surface sites by newly adsorbed water layers is much less important relative to that by the first monolayer. Therefore, as demonstrated in Figure 4, the marked negative correlation of the γ at low humidity (RH $\leq$ 21%) and insignificant dependence at higher RH were observed.

Similar relationship between the γ and RH was found for H_2O_2 uptake on TiO_2 where increasing coverage of water inactivated the surface and thus retarded H_2O_2 uptake.[13] However, in the case of authentic dust aerosols the opposite trend was observed, reflecting a different surface characteristic of authentic dust from oxides. As suggested by Pradhan et al., the adsorption into liquidlike water on authentic dust aerosols dominated H_2O_2 uptake, thus the increasing coverage of water promoted H_2O_2 uptake.[14]

Mechanisms for Heterogeneous Reactions of H_2O_2 on SiO_2 and α-Al_2O_3. On the basis of the experimental results and literature data, the potential mechanisms for heterogeneous decomposition of H_2O_2 on SiO_2 and α-Al_2O_3 are elucidated.

SiO_2 is generally considered to be an inactive oxide, on which various gas species molecularly adsorb. However, H_2O_2 is quite reactive and thermally instable, thus thermal decomposition of H_2O_2 occurs on SiO_2 surfaces, probably via the reactions R1−R3.[21]

$$H_2O_2 + [M] \rightarrow 2OH + [M] \quad (R1)$$

$$OH + H_2O_2 \rightarrow H_2O + HO_2 \quad (R2)$$

$$HO_2 + HO_2 \rightarrow H_2O_2 + O_2(g) \quad (R3)$$

Here, [M] represents the surface sites on oxides.

As discussed above, catalytic decomposition of H_2O_2 can occur on α-Al_2O_3 surface due to its high intrinsic surface reactivity. The catalytic decomposition on α-Al_2O_3 can be initiated by the formation of a surface complex of H_2O_2 with surface OH groups (reaction R4),[26,29] which can undergo reaction R5 to produce a hydroperoxyl radical. In addition, the basic O sites on α-Al_2O_3 may have the potential to decompose H_2O_2 through reaction R6. Furthermore, the surface Al sites, namely oxygen vacancies, may be assumed to be reductive and thereby are expected to react with H_2O_2 via reaction R7.

$$H_2O_2 + [M]OH \leftrightarrow [M]OH - H_2O_2 \quad (R4)$$

$$[M]OH - H_2O_2 \rightarrow [M] + \cdot OOH_{ads} + H_2O \quad (R5)$$

$$[M]O + H_2O_{2(ads)} \rightarrow [M]OH + \cdot OOH_{ads} \quad (R6)$$

$$[M] + H_2O_{2(ads)} \rightarrow [M]OH + \cdot OH_{ads} \quad (R7)$$

As hydroxyl and hydroperoxyl radicals produced during the reactions are highly reactive, they can react immediately with H_2O_2 and other species on the surface,[26,29] via reactions R8 and R9. Finally, these radicals may also react with each other, terminating the reactions R10 and R11.

$$[M] + H_2O_{2(ads)} + \cdot OH_{ads} \rightarrow [M]OH + \cdot OOH_{ads} + H_2O \quad (R8)$$

$$[M]OH + \cdot OOH_{ads} \rightarrow [M] + H_2O + O_2(g) \quad (R9)$$

$$\cdot OOH_{ads} + \cdot OOH_{ads} \rightarrow H_2O_{2(ads)} + O_2(g) \quad (R10)$$

$$\cdot OOH_{ads} + \cdot OH_{ads} \rightarrow H_2O + O_2(g) \quad (R11)$$

The mechanism presented above shows that adsorbed hydroperoxyl radicals are the important intermediates during the reaction. However, no significant infrared absorbance attributed to these radicals was observed during T-FTIR measurements (Figure 1). This is probably due to the rapid consumption of the radicals, resulting in the insufficient surface accumulation for FTIR detection. Besides, the observation of oxygen production in this work is also precluded by experimental constraints.

Atmospheric Implications. Compared to the gas-phase loss processes of H_2O_2 such as photolysis, the role of heterogeneous uptake on silica and alumina particles as a sink for ambient H_2O_2 is probably limited. However, it seems that uptake of H_2O_2 on both mineral oxides plays a significant role in processing mineral aerosols. The heterogeneous uptake of H_2O_2 appears to represent a new source of the oxidants on the surface of mineral aerosols. It is found that H_2O_2 can molecularly adsorb and thermally/catalytically decompose on mineral oxides. The heterogeneous decomposition of H_2O_2, as well as the photolysis of molecularly adsorbed H_2O_2, can lead to the generation of hydroxyl radicals, which may promote the heterogeneous oxidation of organic compounds adsorbed on mineral aerosols. Furthermore, it has been proved that H_2O_2 can substantially contribute to the sulfate formation in liquid aerosol [4,5] and on ice surface,[30,31] thus the considerable amount of molecularly adsorbed H_2O_2 may also be able to facilitate the heterogeneous sulfate formation on mineral aerosols. However, up to date, there have been no experimental studies regarding the oxidation of

adsorbed SO_2 by H_2O_2 on mineral aerosols, thus further studies are required.

It is well known that atmospheric particulate matter (PM) can cause adverse health effects. One proposed mechanism of PM-mediated health effects is the generation of reactive oxygen species such as hydroxyl radical and H_2O_2, followed by oxidative stress.[32] Generally, a hydroxyl radical is considered as being more harmful to health than H_2O_2 and can result in a variety of oxidative damage to cell DNA, as well as membrane lipids and proteins.[33] The heterogeneous uptake of H_2O_2 on mineral aerosols not only leads to an appreciable level of surface adsorbed H_2O_2 but also may generate hydroxyl radicals. Moreover, after entering into the respiratory system, surface adsorbed H_2O_2 may be still capable of serving as the precursor of hydroxyl radicals. Therefore, the heterogeneous uptake of H_2O_2 seems to enhance the potential adverse health effects of mineral aerosols, which should be taken into account in the study of the health effects of PM.

■ ASSOCIATED CONTENT

Supporting Information. Detailed description of the generation of gaseous H_2O_2, and the calibration of integrated absorbance of infrared absorption bands. This material is available free of charge via the Internet at http://pubs.acs.org.

■ AUTHOR INFORMATION

Corresponding Author
*E-mail: zmchen@pku.edu.cn.

■ ACKNOWLEDGMENT

The authors gratefully thank the National Natural Science Foundation of China (grants 40875072 and 21077003) and the State Key Laboratory of Environment Simulation and Pollution Control (special fund) for financial support.

■ REFERENCES

(1) Gunz, D. W.; Hoffmann, M. R. Atmospheric chemistry of peroxides: a review. *Atmos. Environ.* **1990**, *24*, 1601–1633.

(2) Lee, M.; Heikes, B. G.; O'Sullivan, D. Hydrogen peroxide and organic hydroperoxide in the troposphere: A review. *Atmos. Environ.* **2000**, *34*, 3475–3494.

(3) Reeves, C. E.; Penkett, S. A. Measurements of peroxides and what they tell us. *Chem. Rev.* **2003**, *103*, 5199–5218.

(4) Calvert, J. G.; Lazrus, A. L.; Kok, G. L.; Heikes, B. G.; Welega, J. G.; Lind, J.; Cantrell, C. A. Chemical mechanism of acid generation in the troposphere. *Nature* **1985**, *317*, 27–35.

(5) Hua, W.; Chen, Z. M.; Jie, C. Y.; Kondo, Y.; Hofzumahaus, A.; Takegawa, N.; Chang, C. C.; Lu, K. D.; Miyazaki, Y.; Kita, K.; et al. Atmospheric hydrogen peroxide and organic hydroperoxides during PRIDE-PRD'06, China: Their concentration, formation mechanism and contribution to secondary aerosols. *Atmos. Chem. Phys.* **2008**, *8*, 6755–6773.

(6) de Reus, M.; Fischer, H.; Sander, R.; Gros, V.; Kormann, R.; Salisbury, G.; Dingenen, R. V.; Williams, J.; Zollner, M.; Lelieveld, J. Observations and model calculations of trace gas scavenging in a dense Saharan dust plume during MINATROC. *Atmos. Chem. Phys.* **2005**, *5*, 1787–1803.

(7) Mao, J.; Jacob, D. J.; Evans, M. J.; Olson, J. R.; Ren, X.; Brune, W. H.; Clair, J. M., St; Crounse, J. D.; Spencer, K. M.; Beaver, M. R.; et al. Chemistry of hydrogen oxide radicals (HOx) in the Arctic troposphere in spring. *Atmos. Chem. Phys.* **2010**, *10*, 5823–5838.

(8) He, S. Z.; Chen, Z. M.; Zhang, X.; Zhao, Y.; Huang, D. M.; Zhao, J. N.; Zhu, T.; Hu, M.; Zeng, L. M. Measurement of atmospheric hydrogen peroxide and organic peroxides in Beijing before and during the 2008 Olympic Games: Chemical and physical factors influencing their concentrations. *J. Geophys. Res.* **2010**, *115*, D17307, doi:10.1029/2009JD013544.

(9) Denter, F. J.; Carmichael, G. R.; Zhang, Y.; Leliveld, J.; Crutzen, P. J. Role of mineral aerosol as a reactive surface in the global troposphere. *J. Geophys. Res.* **1996**, *101*, 22869–22889.

(10) Falkovich, A. H.; Schkolnik, G.; Ganor, E.; Rudich, Y. Adsorption of organic compounds pertinent to urban environments onto mineral dust particles. *J. Geophys. Res.* **2004**, *109*, D02208, doi:10.1029/2003JD003919.

(11) Usher, C. R.; Michel, A. E.; Grassian, V. H. Reactions on mineral dust. *Chem. Rev.* **2003**, *103*, 4883–4939.

(12) Kolb, C. E.; Cox, R. A.; Abbatt, J. P. D.; Ammann, M.; Davis, E. J.; Donaldson, D. J.; Garrett, B. C.; George, C.; Griffiths, P. T.; Hanson, D. R.; et al. An overview of current issues in the uptake of atmospheric trace gases by aerosols and clouds. *Atmos. Chem. Phys. Discuss* **2010**, *10*, 11139–11250.

(13) Pradhan, M.; Kalberer, M.; Griffiths, P. T.; Braban, C. F.; Pope, F. D.; Cox, R. A.; Lambert, R. M. Uptake of gaseous hydrogen peroxide by submicrometer titanium dioxide aerosol as a function of relative humidity. *Environ. Sci. Technol.* **2010**, *44*, 1360–1365.

(14) Pradhan, M.; Kyriakou, G.; Archibald, A. T.; Papageorgiou, A. C.; Kalberer, M.; Lambert, R. M. Heterogeneous uptake of gaseous hydrogen peroxide by Gobi and Saharan dust aerosols: a potential missing sink for H_2O_2 in the troposphere. *Atmos. Chem. Phys.* **2010**, *10*, 7127–7136.

(15) Chen, Z. M.; Jie, C. Y.; Li, S.; Wang, C. X.; Xu, J. R.; Hua, W. Heterogeneous reactions of methacrolein and methyl vinyl ketone: Kinetics and mechanisms of uptake and ozonolysis on silicon dioxide. *J. Geophys. Res.* **2008**, *113*, D22303, doi:10.1029/2007JD009754.

(16) Ballinger, T. H.; Yates, J. T. IR spectroscopic detection of Lewis acid sites on Al_2O_3 using adsorbed CO. Correlation with Al-OH group removal. *Langmuir* **1991**, *7*, 3041–3045.

(17) Żegliński, J.; Piotrowski, G. P.; Piekoś, R. A study of interaction between hydrogen peroxide and silica gel by FTIR spectroscopy and quantum chemistry. *J. Mol. Struct.* **2006**, *794*, 83–91.

(18) Miller, R. L.; Hornig, D. F. Infrared spectrum and force field of crystalline hydrogen peroxide. *J. Chem. Phys.* **1961**, *34*, 265–272.

(19) Lannon, J. A.; Verderame, F. D.; Anderson, R. W., Jr. Infrared spectrum of solid and matrix-isolated H_2O_2 and D_2O_2. *J. Chem. Phys.* **1971**, *54*, 2212–2223.

(20) Zhao, Y.; Chen, Z. M.; Zhao, J. N. Heterogeneous reactions of methacrolein and methyl vinyl ketone on α-Al_2O_3 particles. *Environ. Sci. Technol.* **2010**, *44*, 2035–2041.

(21) Hiroki, A.; LaVerne, J. A. Decomposition of hydrogen peroxide at water-ceramic oxide interfaces. *J. Phys. Chem. B* **2005**, *109*, 3364–3370.

(22) Mogili, P. K.; Kleiber, P. D.; Young, M. A.; Grassian, V. H. Heterogeneous uptake of ozone on reactive components of mineral dust aerosol: An environmental aerosol reaction chamber study. *J. Phys. Chem. A* **2006**, *110*, 13799–13807.

(23) Knozinger, H.; Ratnasamy, P. Catalytic aluminas: surface models and characterization of surface sites. *Catal. Rev.—Sci. Eng.* **1978**, *17*, 31–70.

(24) Michel, A. E.; Usher, C. R.; Grassian, V. H. Reactive uptake of ozone on mineral oxides and mineral dusts. *Atmos. Environ.* **2003**, *37*, 3201–3211.

(25) Goodman, A. L.; Bernard, E. T.; Grassian, V. H. Spectroscopic study of nitric acid and water adsorption on Oxide particles: enhanced nitric acid uptake kinetics in the presence of adsorbed water. *J. Phys. Chem. A* **2001**, *105*, 6443–6457.

(26) Lin, S. S.; Gurol, M. D. Catalytic decomposition of hydrogen peroxide on iron oxide: Kinetics, mechanism, and implications. *Environ. Sci. Technol.* **1998**, *32*, 1417–1423.

(27) Al-Abadleh, H. A.; Grassian, V. H. FT-IR study of water adsorption on aluminum oxide surfaces. *Langmuir* **2003**, *19*, 341–347.

(28) Eng, P. J.; Trainor, T. P.; Brown, G. E., Jr; Waychunas, G. A.; Newville, M.; Sutton, S. R.; Rivers, M. L. Structure of the Hydrated α-Al_2O_3 (0001) Surface. *Science* **2000**, *288*, 1029–1033.

(29) Do, S. H.; Batchelor, B.; Lee, H. K.; Kong, S. H. Hydrogen peroxide decomposition on manganese oxide (pyrolusite): Kinetics, intermediates, and mechanism. *Chemosphere* **2009**, *75*, 8–12.

(30) Chu, L.; Diao, G. W.; Chu, L. T. Heterogeneous Interaction of SO_2 on H_2O_2-Ice Films at 190−210K. *J. Phys. Chem. A* **2000**, *104*, 7565–7573.

(31) Clegg, S. M.; Abbatt, J. P. D. Uptake of gas-phase SO_2 and H_2O_2 by ice surfaces: Dependence on partial pressure, temperature, and surface acidity. *J. Phys. Chem. A* **2001**, *105*, 6630–6636.

(32) Shen, H.; Barakat, A. I.; Anastasio, C. Generation of hydrogen peroxide from San Joaquin Valley particles in a cell-free solution. *Atmos. Chem. Phys.* **2011**, *11*, 753–765.

(33) Valavanidis, A.; Fiotakis, K.; Vlachogianni, T. Airborne particulate matter and human health: Toxicological assessment and importance of size and composition of particles for oxidative damage and carcinogenic mechanisms. *J. Environ. Sci. Health, Part C* **2008**, *26*, 339–362.